FLAT-PLATE TRANSITION

Barbara A. Ercegovic
National Aeronautics and Space Administration
Lewis Research Center
Cleveland, Ohio 44135

A heat transfer workshop held at Lewis in 1980 highlighted the need for more transition research. Therefore in 1981 we began a new research effort to build a boundary-layer transition tunnel. This facility only recently became operational. The data obtained so far are merely qualitative. The main goal is to predict heat transfer given any combination of factors such as pressure gradient, turbulence level, Reynolds number, or intermittency factor.

The boundary-layer transition tunnel (fig. 1) is a closed-loop tunnel that controls the turbulence level, velocity, and temperature of the air within it. We may add the ability to control the unsteadiness. The lid of the test section is hinged and can be raised or lowered to set the test-section pressure gradient. The initial test surface is adiabatic, but we anticipate use of a heated or cooled test surface for investigating the effects of roughness or even curvature. The circuit (fig. 2) consists of a blower, a flow-conditioning box, a test section, a diffuser section, a damper valve, and an air heater. The return leg consists of an air filter box and a heat exchanger. The tunnel is essentially at atmospheric pressure, since the blower has a capacity of only about 3 kPa (12 in of H_2O). We can vary the air temperature within the tunnel from about 15 to 65 °C (60 to 150 °F), but any given run is done at isothermal conditions. We will be testing over the velocity range 3.5 to 35 m/sec (10 to 100 ft/sec). The pressure gradient can be adjusted anywhere from adverse to favorable. The test section has a cross section 15.5 cm high by 69 cm wide by 1.53 m long (6 in by 27 in by 5 ft). The static pressure distribution can be measured across the entire test surface. Thirty taps are located along the centerline 20 cm (8 in) on either side of center, with a slight concentration at the leading edge of the plate (fig. 3). The test surface is also instrumented with flush-mounted hot-film sensors, which are used to detect the transition. The hot-film sensors are concentrated along the centerline, with a few 15.5 cm (6 in) off center (fig. 4). Most centerline sensors are spaced 5.1 cm (2 in) apart.

A major problem with this facility has been the flow distribution along the tunnel cross section. Because of the blower exit geometry there is a high degree of nonuniformity in the flow field. Figure 5 shows contour lines at the exit of the blower, before the flow-conditioning box. Each line is a line of constant velocity. The goal was a variation from the mean velocity of no more than ± 2 percent. As shown, the pattern is very nonuniform at this location. The flow-conditioning box uses perforated plates, screens, baffles, and "soda straws" to straighten out the flow. At the exit to the flow-conditioning box (fig. 6), going into the contraction, the flow distribution is greatly improved. To achieve various levels of turbulence, four sets of grids (table I) can be inserted into the flow-conditioning box, one at a time. The grids go from fine (1) to coarse (4). The percentage of open area ranges from 61 to 65 percent. Turbulence intensities range from 0.46 percent with no grid

to 5.46 percent with the coarsest grid. This is for a free-stream velocity of about 16.8 m/sec (55 ft/sec).

A continuous oscilloscope trace of one sensor located on the centerline about 45 cm (18 in) from the leading edge (fig. 7) shows Tollmien-Schlichting waves. The free-stream velocity in this case was 17.7 m/sec (58 ft/sec). The frequency of these disturbances was about 225 Hz, which is in the range of the Tollmien-Schlichting disturbance. Upstream sensors showed purely laminar flow with lower amplitudes in the disturbance. Downstream sensors showed higher amplitudes and occasional turbulent bursts. Figure 8 shows traces of sensors 1, 2, 5, and 6, which are consecutive along the centerline of the test section. A turbulent burst is just entering upon sensor 1. It moves downstream and is picked up by the other sensors. The burst enlarges as it moves downstream. Figure 9 shows an oscilloscope trace of sensor 1, which is the first sensor on the centerline. The other three traces are for sensors 26, 27, and 28, which are the first three to the left of the centerline. A turbulent burst approaches sensor 26, moves on to sensors 27 and 28, and breaks down into turbulence. Since the turbulence does not appear on sensor 1, whatever is on sensor 1 does not necessarily show up on sensor 26.

The remainder of the information contained herein is only qualitative and gives an idea of the type of data we will be able to obtain. Figure 10 shows the intermittency factor as a function of X, where intermittency is defined as the fraction of time that the flow is turbulent at any given location. For an intermittency factor of 1 the flow is fully turbulent. At the lowest Reynolds number and $X = 56$ cm (21 in), the intermittency factor is just beginning to increase above the zero (laminar) level. As the Reynolds number increases, this initial increase in intermittency factor moves upstream. Therefore as the Reynolds number increases, the onset of transition occurs earlier. Figure 11 is a plot of the rms fluctuating output divided by the relative dc output as a function of X. The y-axis variable is a qualitative representation of the level of the fluctuation; it gives the starting location and shows the length of the transition zone. The voltage peaks within the transition region. At the lowest Reynolds number, about 300 000, the voltage begins to increase at $X = 56$ cm (21 in) but has not yet peaked. At a Reynolds number of 428 000, the voltage has begun to pick up, has peaked, and is dropping again at $X = 56$ cm (21 in). At the highest Reynolds number, 500 000, at $X = 10$ cm (4 in), the fluctuating voltage starts at a higher level, peaks, and then drops off and remains fairly constant at a level higher than that before the transition. Figure 12 is a plot of intermittency factor as a function of X for a unit Reynolds number of 1 500 000/m (490 000/ft). The pressure gradient K was varied within the test section by changing the position of the lid. For $K = 0$ the intermittency is about 0.22 (i.e., transition has already started). At $X = 31$ cm (12 in), the flow is fully turbulent. For accelerated flow (i.e., positive values of K), transition is delayed downstream (e.g., for $K = 13.8 \times 10^{-8}$). For decelerated flow (i.e., negative values of K), the starting point of the transition moves upstream, and the flow becomes fully turbulent at successively earlier locations on the flat plate. Figure 13 is a plot of the same data with the rms voltage over the dc output as a function of X. Again, for $K = 0$ the flow has already started into transition at $X = 15.5$ cm (6 in) since it has peaked and dropped off. As K becomes positive, transition is delayed. As K becomes negative, the start of transition is pushed much farther upstream. The initial increase in the fluctuating voltage occurs at successively smaller values of X as K becomes increasingly negative.

TABLE I. - TURBULENCE LEVELS DOWNSTREAM OF CONTRACTION

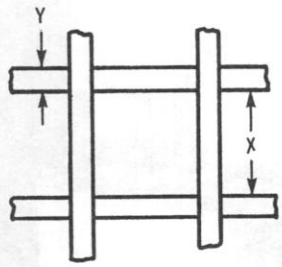

Grid	Ratio of space to width of bar, X/Y	Open area, percent of total area	Turbulence, percent
0	(a)	100	0.46
1	0.69/0.19	62	.98
2	2.06/0.50	65	2.06
3	5.50/1.50	62	4.58
4	7.00/2.00	61	5.46

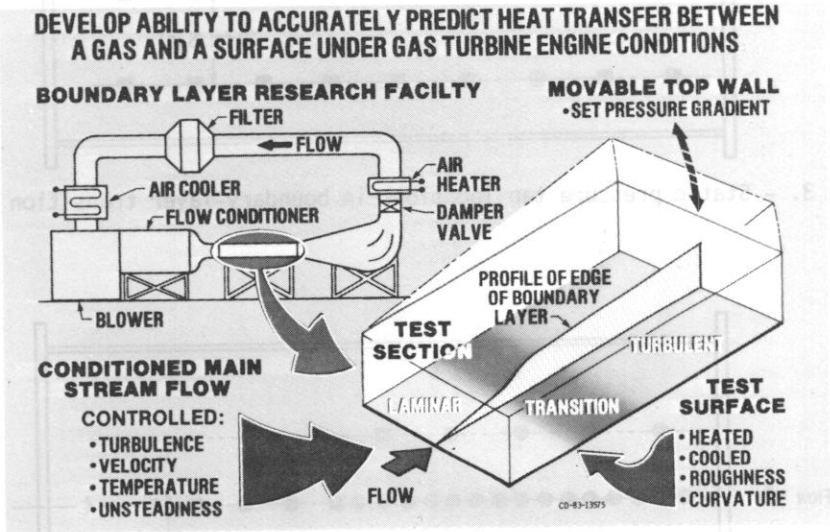

Figure 1. - Boundary-layer research.

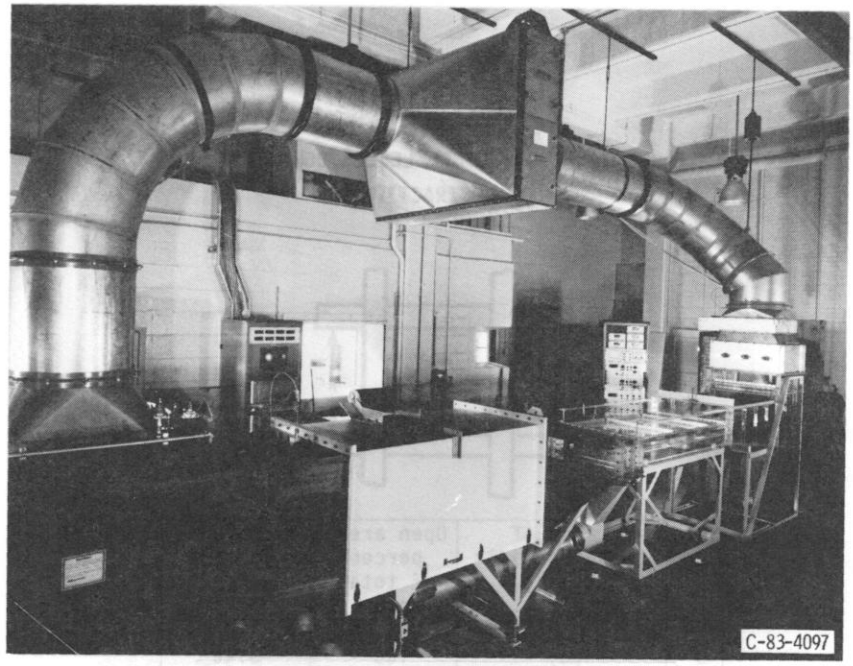

Figure 2. - Test facility.

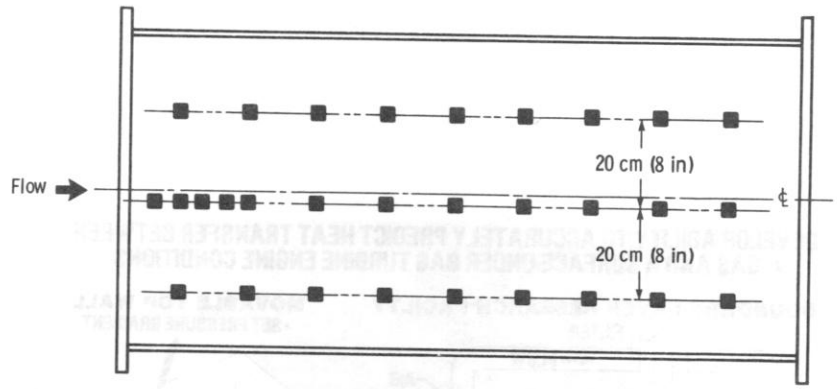

Figure 3. - Static pressure tap locations in boundary-layer transition tunnel.

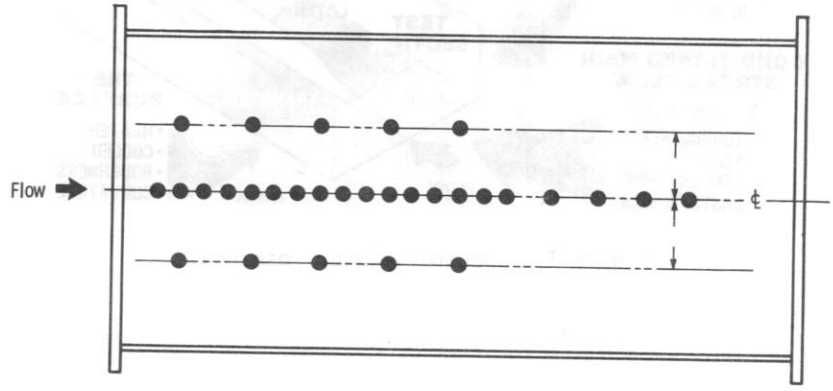

Figure 4. - Thin-film sensor locations in boundary-layer transition tunnel.

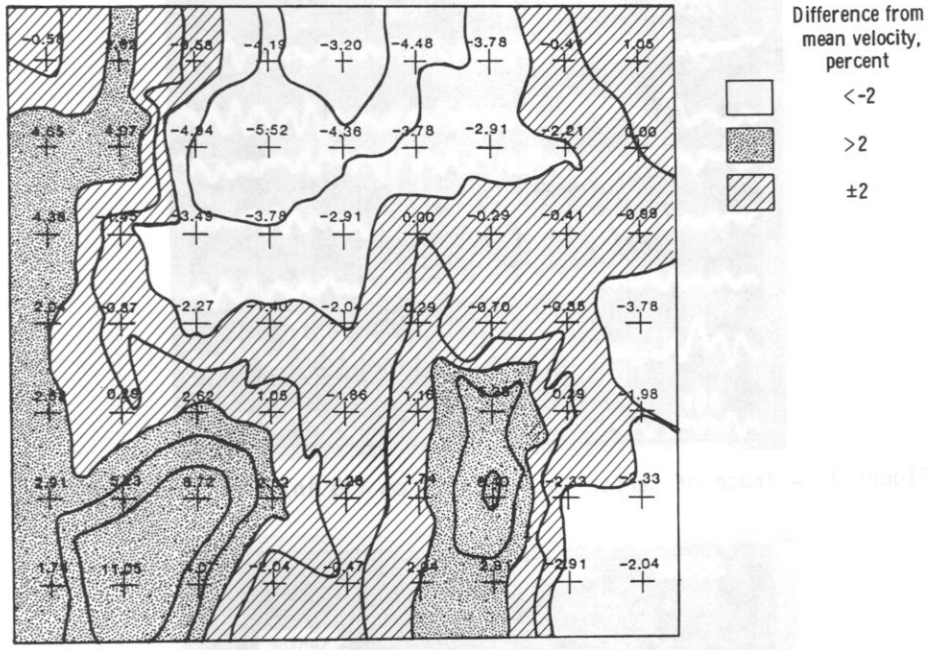

Figure 5. - Contour lines at blower exit.

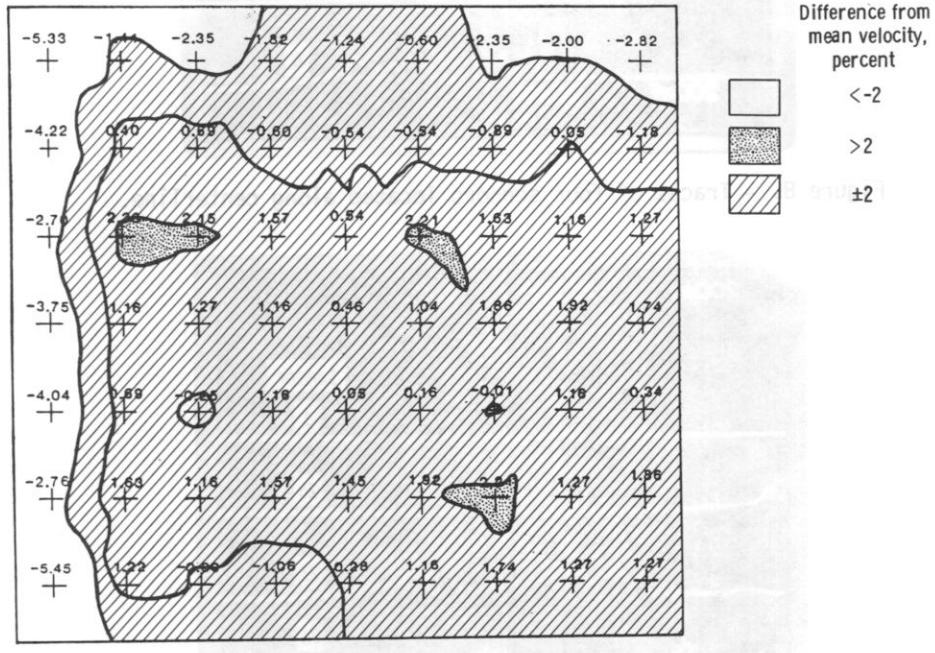

Figure 6. - Contour lines at exit of flow-conditioning box.

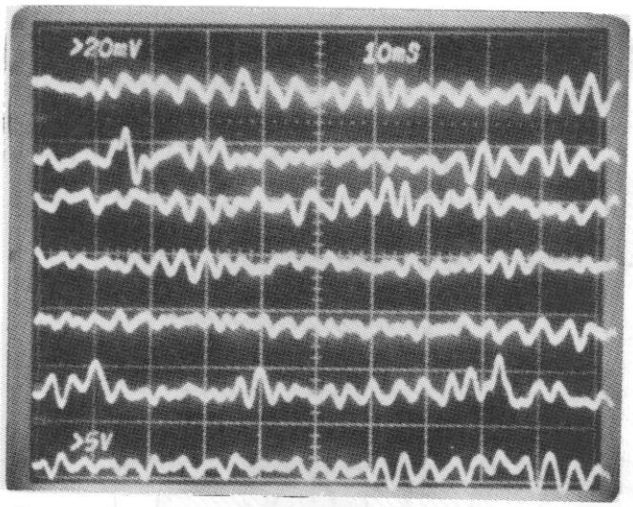

Figure 7. - Trace of sensor located 45.7 cm (18 in) from leading edge.

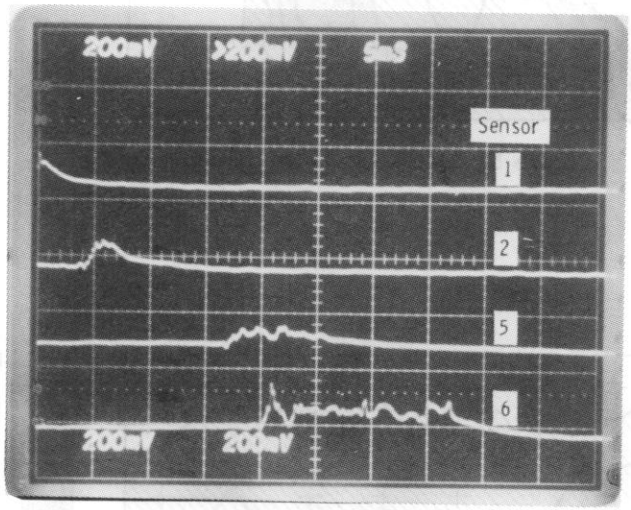

Figure 8. - Traces of four sensors located along centerline.

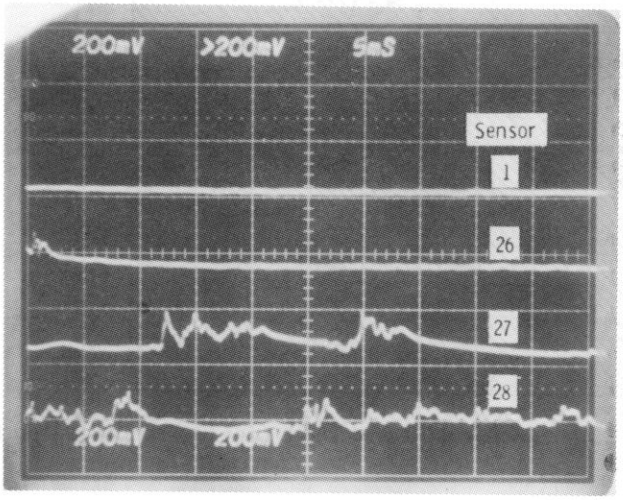

Figure 9. - Traces of four sensors on and to left of centerline.

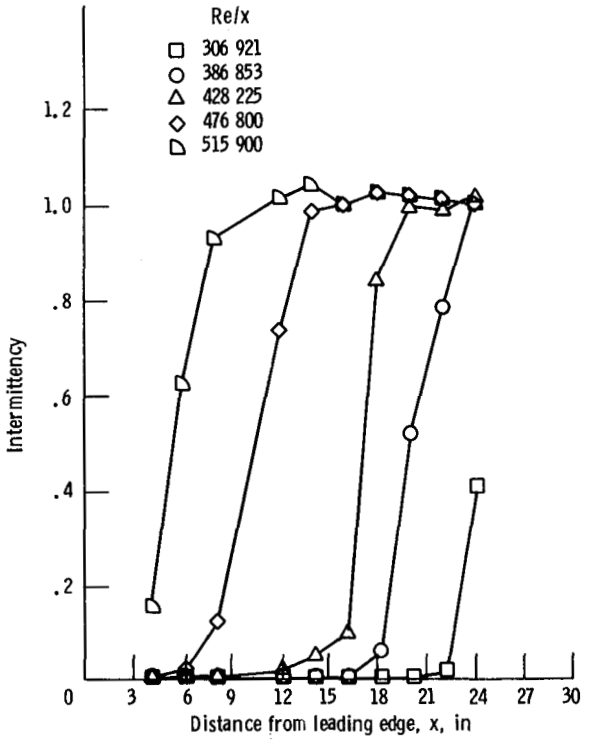

Figure 10. - Intermittency as function of distance from leading edge.

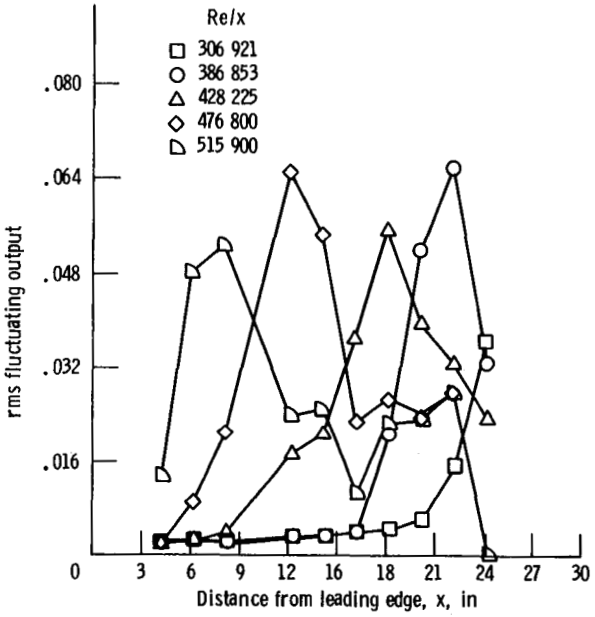

Figure 11. - rms fluctuating output as function of distance from leading edge.

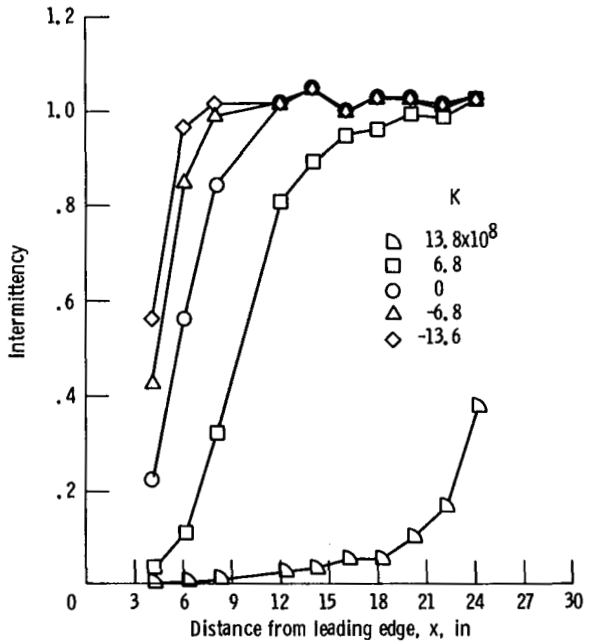

Figure 12. - Intermittency as function of distance from leading edge for Re/x = 490 000.

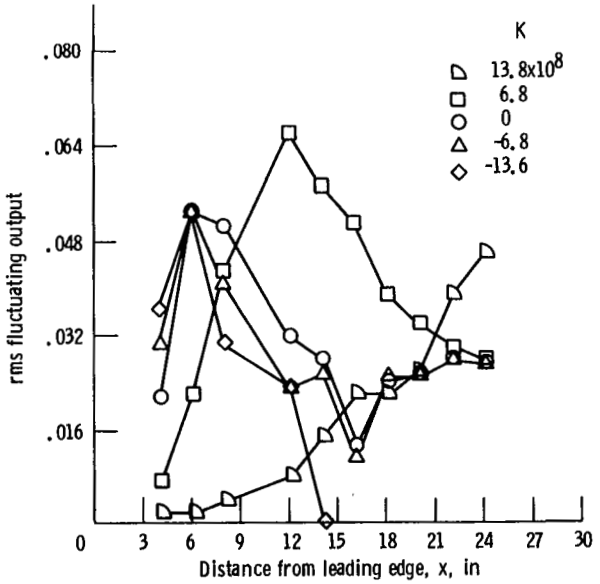

Figure 13. - rms fluctuating output as function of distance from leading edge for Re/x = 490 000.